

Full Length Article

Molecular simulation of thermodynamic properties of CH₄ and CO₂ adsorption under different moisture content and pore size conditions

Ziwen Li, Yansong Bai*, Hongjin Yu, Hongqing Hu, Yinji Wang

College of Safety and Emergency Management Engineering, Taiyuan University of Technology, Taiyuan 030024, PR China



ARTICLE INFO

Keywords:

Moisture content
Molecular simulation
CO₂ displacement of CH₄
Wall superimposed effect
Adsorption potential

ABSTRACT

In order to further clarify the thermodynamic properties of CH₄ and CO₂ adsorption in coal, a Monte Carlo method with a giant regular system was used to simulate the adsorption behavior of CH₄ and CO₂ in coal at different moisture contents and pore sizes. The results show that the adsorption of CH₄ and CO₂ in coal molecules is negatively correlated with the moisture content. As the pore size increases, the wall superimposed effect decreases, the stability of adsorption becomes less stable, and the selectivity of CO₂ adsorption decreases, but the space to accommodate gas molecules becomes larger, which makes the adsorption amount rise. The average heat of adsorption of CH₄ and CO₂ showed a decreasing and then increasing relationship with the moisture content, and a negative correlation with the pore size, and the effect of H₂O on CO₂ is stronger than that of CH₄. With the increase of moisture content, the absolute value of adsorption energy increases overall, and the high potential of water clusters tends to attract CO₂ molecules more. With the increase of pore size, the wall superimposed effect weakens and the adsorption stability becomes worse, which makes the absolute value of adsorption energy smaller. The overall adsorption entropy of CH₄ and CO₂ has a negative correlation with moisture content and a positive correlation with pore size. The comparison of the slope of the fitted curves of adsorption entropy at different moisture contents adds that CO₂ mainly displaces CH₄ molecules in the middle of the pores at 3% moisture content.

1. Introduction

Coalbed methane (CBM) is an unconventional natural gas, mainly produced during coalification, which is endowed in coal seams in an adsorbed state [1–3]. According to the International Energy Agency (IEA), China's CBM reserves are as high as 36.8 trillion cubic meters, ranking third in the world [4], and it is the most realistic and reliable unconventional oil and gas resource in China at present. Therefore, it is an urgent need for the country to continuously make technological breakthroughs in efficient exploration and development of coalbed methane. In addition, the global greenhouse effect is intensifying, and greenhouse gas emission reduction is of great concern. CH₄ is a serious greenhouse gas, and the greenhouse effect caused by the same volume is 20–25 times that of CO₂, so CH₄ emission reduction is an important part of air pollution prevention and control, and the efficient extraction and utilization of coalbed methane is a curative solution for coalbed methane emission reduction. At present, the efficient extraction technologies of CBM mainly include hydraulic fracturing technology [5–7], multi-branch horizontal well technology [8], heat injection and

production enhancement technology [9,10] and gas injection and production enhancement technology [11,12]. Among them, CO₂-enhanced coalbed methane technology (CO₂-ECBM) combines carbon sequestration and enhanced coalbed methane recovery with multiple economic, resource and environmental benefits of promoting natural gas development and reducing greenhouse gas emissions [13], and carbon capture and storage (CCS) is a key decarbonization technology to achieve carbon neutrality in China, so it is of great importance to carry out research on CO₂-ECBM technology.

CO₂-ECBM has been explored and practiced worldwide for many years. In 1995, the earliest and largest CO₂-ECBM pilot project was established in the northern San Juan Basin in the United States, including four CO₂ injection wells and 16 CBM production wells [14]. CO₂-ECBM attempts were carried out in Alberta, Canada [15], Yubari, Hokkaido, Japan [16], Upper Silesian Basin, Poland [17], and Verene coalfield, Slovenia [18], etc. In 2004, a CO₂-ECBM pilot test was carried out in the southern part of Qingshui basin in China, and the production and recovery rate of CBM per well were significantly improved [19]. These past projects can demonstrate the feasibility of CO₂-ECBM and

* Corresponding author.

E-mail address: baiyansong1620@link.tyut.edu.cn (Y. Bai).

reveal some of the problems faced in project implementation. In order to solve these problems, we need to study the adsorption of CH₄ and CO₂ in coal. Zuber et al. experimentally verified that the phenomenon of increased methane production can be achieved by injecting CO₂ into coal seams [20]. Bustin suggested that methane desorption from coal seams can be induced by injecting non-methane gas into the coal seam to reduce the partial pressure of methane in the free gas or to compete with it for adsorption space [21]. Fulton et al. conducted an experimental study of carbon dioxide injection at low pressure to replace methane gas in dry coal and saturated water wet coal samples, and the results showed that the methane recovery rate increased by 9 %–57 % compared to the natural emission rate after carbon dioxide injection, and they concluded that the enhanced methane recovery technique of carbon dioxide recirculation injection is the most effective way to regain the adsorbed methane gas in coal [22]. Reznik et al. carried out a pilot study on methane replacement by carbon dioxide injection under high pressure based on Fulton, and all the methane was replaced in the coal samples, and they also carried out a test on methane replacement by a mixture of CO₂/N₂ [23]. Some other studies [24–28] focused on the effect of different properties of coal on the adsorption capacity of CO₂ and CH₄, such as moisture, minerals, ash and volatiles, for example, the adsorption capacity of coal for CH₄ and CO₂ is negatively correlated with ash content and the mineral content will contribute to additional CO₂ adsorption.

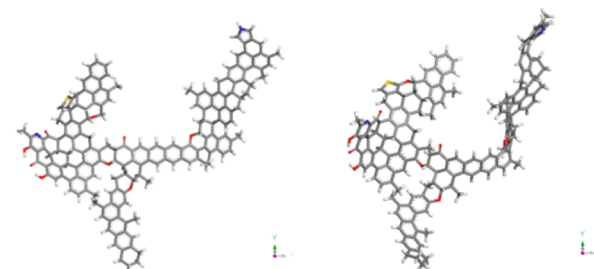
In addition to experimental means, molecular simulations are beginning to emerge in studying the adsorption behavior of CO₂ and CH₄ on coal, and several authors have carried out studies using molecular dynamics (MD), Monte Carlo simulation (MC), and density flooding theory (DFT) [29–33]. Most simulations showed that CO₂ preferentially adsorbs over CH₄, where CO₂ has a higher adsorption selectivity than CH₄. Y. Dang et al. concluded that CO₂ has a higher electrostatic force and prefers to adsorb in micropores, making CO₂ exhibit a higher adsorption affinity than CH₄ [30]. J. Zhang et al. found that at a given temperature and for a given type of coal, the adsorption selectivity depends on pressure and molar fraction of CO₂ [34]. However, the selectivity varies with pressure for different coals. In some cases, the selectivity is greatest at low pressures and decreases with increasing pressure [30,31], while in other cases the selectivity increases gradually with pressure [32]. The CO₂/CH₄ adsorption selectivity decreases with coal rank and increases with increasing oxygen-containing functional groups [31]. Cracknell et al. simulated the adsorption of molar mixtures such as CH₄/C₂H₆ in graphite slit pores and found that the selection of the gas molecular model significantly affects the selective adsorption of gas molecules by the adsorbent [35,36]. You et al. used GCMC simulation method for the adsorption of CH₄, CO₂, H₂O, and N₂ and obtained their adsorption enthalpies [37–39]. In addition, the moisture in the coal makes the adsorption selectivity fluctuate with coal grade, so the optimal moisture content of CO₂-ECBM depends on the coal grade [31].

From the current status of research on the adsorption properties of CH₄ and CO₂ in coal, it is mainly experimental and centered on aspects such as competitive adsorption, while the application of molecular simulations mainly involves evaluation indexes such as adsorption selectivity and enthalpy change of adsorption, and the research on the mechanism of competitive adsorption and co-adsorption of CH₄/CO₂ still suffers from the lack of basic thermodynamic data and the lack of in-depth research on intermolecular interactions [40]. The inner surface of the coal seam is porous and usually contains water, and both water and pore size have significant effects on gas adsorption in the coal seam. In addition, the gas adsorption process is often accompanied by changes in thermodynamic energy, and the study of the thermodynamic properties on coal adsorption of multi-component gases can further clarify the mechanism of interaction between coal and gas phases. However, there are few researches on the thermodynamic properties of CH₄ and CO₂ adsorption under different water content and pore size conditions were considered. Therefore, in this paper, the GCMC method was used to compare the single- and two-component injections of CH₄ and CO₂

Table 1

Structural parameters of the No. 8 coal plane model from Malan [37].

Molecular Formula	Molecular mass	Elemental content/%				
		C	H	O	N	S
C ₁₇₉ H ₁₂₆ O ₁₀ N ₂ S	2494	86.13	5.05	6.42	1.12	1.28



(a) Geometrically optimized (b) Annealed coal molecular model

Fig. 1. Geometrically optimized and annealed coal molecular model.

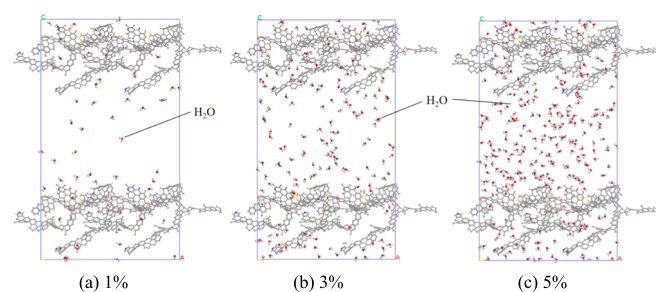


Fig. 2. Slit model for different moisture content.

under different moisture content and pore size by means of molecular simulations. The results are then analyzed for adsorption thermodynamic properties to investigate the effects of different moisture content and pore size on gas adsorption and to provide some theoretical support for CO₂-ECBM technology.

2. Construction of coal molecular model and simulation scheme

2.1. Construction of the coal molecular model and parameter settings

The author conducted a simulation study based on the macromolecular structure of Maran 8 coal in the literature [41], and the maximum vitrinite reflectance of Malan No. 8 coal is 1.205 %, which is a high quality fatty fine coal in China and is the main coal type for coking coal preparation. The relevant parameters of this structure are shown in Table 1.

The molecular structure of coal was modeled using Material studio 2019, and molecular mechanics and dynamics were optimized using the Forceite module. Molecular mechanics optimization parameters were set as follows: Geometry Optimization for the task, COMPASS for the force field, Charge using QEq for the charge calculation. Molecular dynamics optimization parameters are set as follows: Anneal for the task, 10 annealing cycles, 300 K for the initial temperature, 500 K for the maximum temperature, NVT system synthesis, the simulation time of 10 ps, the temperature control method is Nose, and the force field is set as above. The optimized model is shown in Fig. 1.

2.2. Modeling of different water contents and different pore sizes

Using the Amorphous Cell module of MS, a crystal cell containing

two coal molecules was built and the density was 1.3 g/cm³. After the optimization of molecular mechanics and dynamics, the cell was cut in the (101) direction. Then 1 nm, 3 nm and 5 nm vacuum layers were added to the Build layers module and supercells of 2 × 2 × 1 were built. Thus, slit models with different aperture sizes were obtained. Using the Sorption module and Locate task item, a certain number of water molecules were adsorbed in advance to build the models of coal molecules with moisture content of 1 %, 3 % and 5 %, as shown in Fig. 2.

2.3. Simulation scheme and parameter settings

The Grand Canonical Ensemble Monte Carlo (GCMC) method was used to simulate the adsorption of CH₄ and CO₂ in coal molecules with different moisture contents and different pore sizes. The Sorption module of MS was used, the task item was selected as Adsorption Isotherm, the force field was selected as COMPASS, the simulation temperature was 318 K, and the pressure was 0.01 ~ 10 MPa. For the simulation of different moisture contents, the adsorbent was a 3 nm coal structure model with different moisture contents. For different pore sizes, the adsorbent was a coal structure model with different pore sizes at 3 % moisture content. Both CH₄ and CO₂ molecules are geometrically optimized and injected in equal proportions.

GCMC simulations yield the number of gas molecules adsorbed in a single cell, which is converted to the experimentally used adsorption volume using Eq. (1).

$$V = 10^3 \times \frac{N}{N_A \times M} \quad (1)$$

where, V is the adsorption volume, mmol/g; N is the number of gas molecules adsorbed in a single cell, moleculars/u.c.; N_A is Avogadro constant, 6.02×10^{23} ; M is the cell unit mass, g.

3. Surface electrostatic potential of different gas molecules

The electrostatic potential distribution (ESP) on the molecular surface is important in the study of molecular interactions [42,43]. In the early stage of chemical reactions, molecules approach each other mainly by electrostatic attraction, and it is usually believed that sites with negative and smaller values of electrostatic potential are more likely to have electrophilic reactions, while sites with positive and larger values of electrostatic potential are more likely to have nucleophilic reactions. By analyzing the surface electrostatic potential distribution of coal molecular model and gas molecules, the strength of interaction between the surface of coal molecular model and gas molecules can be judged, and the adsorption mechanism of gas molecules on the surface of coal molecules can be reasonably explained. Before specifically analyzing the adsorption characteristics of CH₄ and CO₂ gases in coal at different moisture contents and pore sizes, the microscopic mechanism of interaction between CH₄ molecules, CO₂ molecules and H₂O molecules was clarified by the electrostatic potential. Some fragments of the macro-molecular model of maranite, with the chemical formula C₂₉H₂₇O₄, were selected, and their surface electrostatic potentials showed negative near the center of benzene ring and oxygen atom, especially the oxygen atom showed strong electro-negativity, while the hydrogen atom at the edge had positive electrostatic potential. The relative positions of molecules and the strength of interactions are analyzed by the electrostatic potential distribution, i.e., regions with positive values of electrostatic potential on the surface of molecules are more inclined to attract regions with negative values, and the regions where interactions occur are stronger if the absolute values of electrostatic potential values are larger. There are more oxygen-containing functional groups in the molecular model of Malan mine, and the oxygen-containing functional groups have an important influence on the generation and adsorption of CBM, so the surface electrostatic potential analysis is carried out for the adsorption configuration of different gas molecules at the oxygen-containing

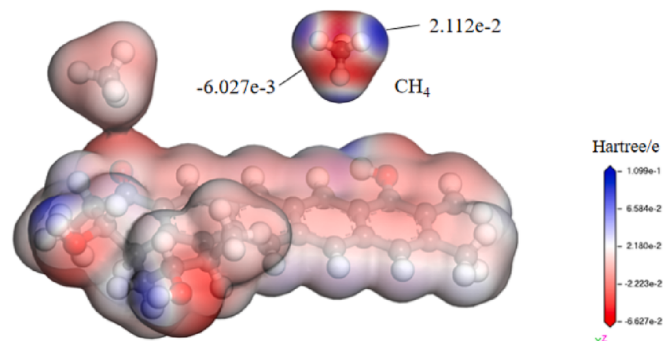


Fig. 3. Adsorption conformation and surface electrostatic potential of CH₄.

functional groups on the coal surface.

CH₄ belongs to sp³ hybridization, and it has no isolated electron pairs and interacts with coal molecules mainly by van der Waals forces [44], its electrostatic potential is positive except near the hydrogen atom, and the rest of the region is negative with a minimal value of -0.006027 and a maximal value of 0.02112 . The adsorption configuration of CH₄ near the oxygen-containing functional group in coal is shown in Fig. 3. The negative electrostatic potential exhibited by the oxygen atom in the coal molecule attracts the hydrogen atoms in CH₄, and the electrostatic potential of both crosses. This crossover can also be called as penetration. CH₄ molecules and coal molecules have a small electrostatic potential penetration volume, which indicates the smaller interaction between the two.

CO₂ belongs to sp hybridization, and each oxygen atom exists as an isolated electron pair with strong electronegativity [44], and the very small value point of the electrostatic potential is at the surface of the oxygen atom, -0.01726 , and the very large value point is near the carbon atom, 0.06298 , whose absolute value is higher than CH₄ and smaller than H₂O. As seen in Fig. 4, the negative electrostatic potential at the oxygen-containing functional group in the coal molecule attracts the carbon atom in the CO₂ molecule so that it adsorbs on the coal surface in a parallel configuration, and the surface electrostatic potential of coal and CO₂ produces a penetration, and the penetration volume is between CH₄ and H₂O, indicating that the interaction between CO₂ molecules and coal is stronger than that of CH₄ and weaker than that of H₂O.

H₂O belongs to sp³ hybridization, there are also two pairs of isolated electron pairs, and as a polar molecule, its electrostatic potential is much stronger than that of CO₂, the electrostatic potential has a very small value of -0.06548 on the surface of oxygen atom and a very large value of 0.09048 on the surface of hydrogen atom. When H₂O molecules are close to each other, the neighboring H₂O molecules will have mutual electrostatic attraction due to polarity, because the negative charge on the isolated electron side of H₂O molecules attracts the hydrogen nuclei of other H₂O molecules, resulting in H₂O molecular clusters. The negative charge on the isolated electron side of the molecule attracts the nuclei of hydrogen atoms in other H₂O molecules, causing hydrogen bonding linkage between H₂O molecules and forming a cluster of H₂O molecules. Hydrogen atoms in H₂O molecules are stably adsorbed at the oxygen-containing functional groups of coal (Fig. 5), and the penetration volume of the electrostatic potential of both is significantly larger than that of CH₄ and CO₂, indicating the strongest interaction between coal and H₂O molecules.

4. Effect of moisture content on the thermodynamic properties of CH₄ and CO₂ adsorption

4.1. Gas adsorption capacity and thermal properties of adsorption

Fig. 7 shows the variation curves of CH₄ and CO₂ adsorption with injection pressure under different water content conditions, which were

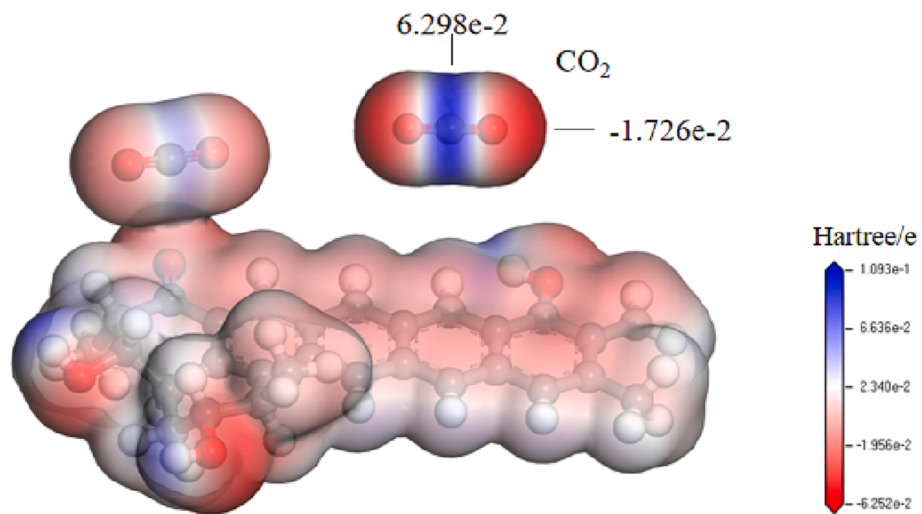
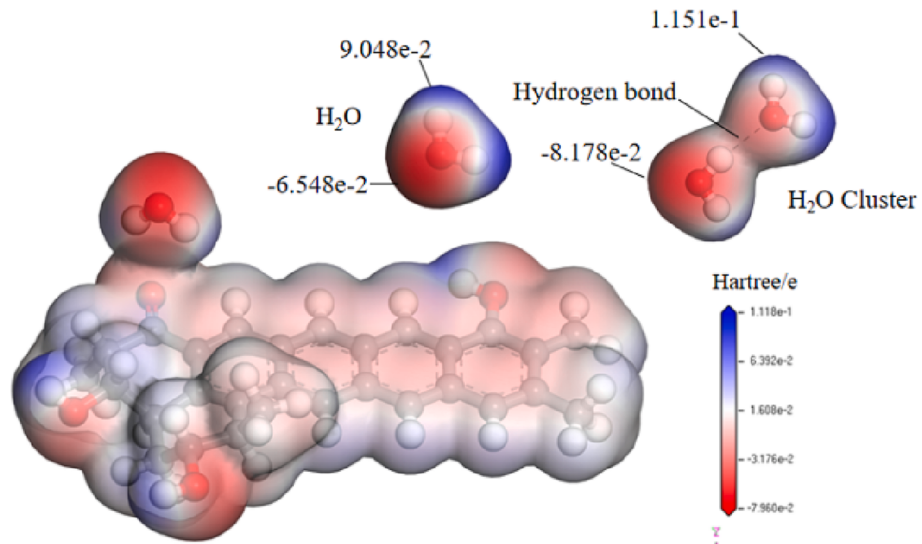
Fig. 4. Adsorption conformation and surface electrostatic potential of CO_2 .Fig. 5. Adsorption conformation and surface electrostatic potential of H_2O .

Table 2
Fitting parameters of Langmuir equation at different moisture content.

Moisture content/%	$a/(\text{mmol/g})$				$b/(\text{MPa}^{-1})$			
	CH_4		CO_2		CH_4		CO_2	
	(a)	(b)	(a)	(b)	(a)	(b)	(a)	(b)
0	33.77	9.87	98.67	87.52	0.11	0.20	0.08	0.03
1	34.94	13.10	91.73	57.47	0.10	0.11	0.08	0.06
3	29.04	6.73	76.93	80.10	0.10	0.26	0.10	0.04
5	30.34	6.24	58.34	59.33	0.08	0.24	0.14	0.05

fitted using the Langmuir equation, and the fitting results are shown in Table 2.

$$V = \frac{abp}{1 + bp} \quad (2)$$

where, p is the pressure, MPa; a is the saturation adsorption amount, mmol/g; b is the adsorption equilibrium parameter, MPa^{-1} .

As can be seen from Fig. 7, the adsorption of single-component CH_4 and CO_2 decreases with the increase of moisture content. From the fitted data, the decrease in the saturation sorption of CO_2 is much more

pronounced compared to CH_4 , so it can be inferred that H_2O affects CO_2 sorption more significantly than CH_4 . When multi-component injection was carried out, the adsorption amount of CH_4 did not change significantly from 0 % to 1 % moisture content, while the adsorption amount of CO_2 decreased significantly. H_2O has the strongest adsorption capacity in coal and will preferentially occupy the high-energy adsorption sites, while CO_2 is mainly adsorbed on the coal surface at this time, and CH_4 is more in the middle of the pores, so H_2O mainly displaces CO_2 on the coal surface, indicating that it is not favorable for CO_2 to displace CH_4 at this time. The adsorption of CH_4 decreases significantly from 1 % to 3 %

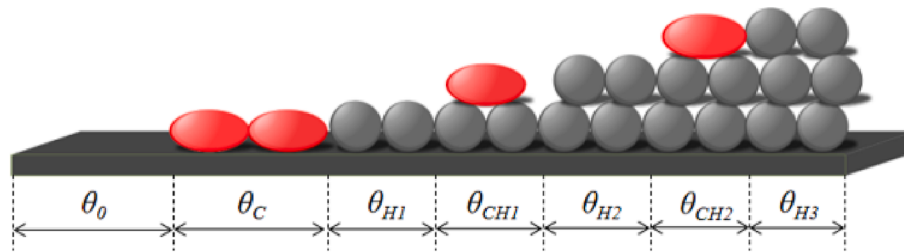


Fig. 6. LBET adsorption model (C for CO_2 , H for H_2O) [43].

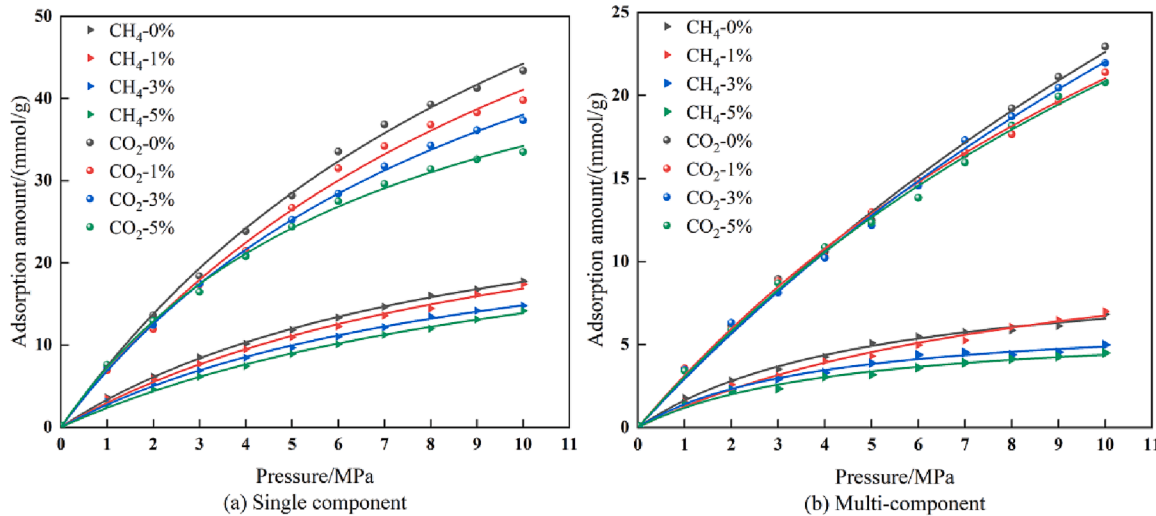


Fig. 7. Isothermal adsorption curves of CH_4/CO_2 at different moisture content.

moisture content, while the adsorption of CO_2 increases. A certain number of H_2O molecules form H_2O clusters [45], and the H_2O clusters attract CO_2 , indicating that this is a favorable time for CO_2 to displace CH_4 . But in previous studies H_2O is usually considered to be unfavorable for CH_4 and CO_2 adsorption. For example, Zhang et al. found that an increase in moisture content significantly weakens the strength of the interaction between gas molecules and coal macromolecules [46], and Billemont et al. found through experiments and molecular simulations that the presence of H_2O causes a linear decrease in the adsorption of gases [47]. However, this is not entirely the case in reality. For example, Qiao et al. found that when the pores of the adsorbent material have their own independent CO_2 binding sites and H_2O binding sites, and they do not overlap, the adsorption of CH_4 is not favored [48], and Li et al. proposed an extended Langmuir-BET (LBET) adsorption model, which considers the synergistic relationship between CO_2 and H_2O molecules, assuming that the easily adsorbed H_2O molecules form an aqueous layer as secondary adsorption sites, and through hydrogen bonding interactions and hydration reactions, etc. to further adsorb CO_2 [49] (Fig. 6). The adsorption amount of CH_4 remained basically the same again from 3 % to 5 % moisture content, and the adsorption amount of CO_2 started to decrease. A large number of H_2O molecules formed a H_2O molecule layer, which hindered the adsorption of CO_2 and CH_4 [50]. Since the coal surface is basically occupied by CO_2 and H_2O molecules when the moisture content is 3 %, the content of CH_4 almost reaches extremely low, and it is mostly in the middle of the pore space, so when the moisture content is 5 %, the H_2O molecular layer is formed, which mainly hinders the adsorption of CO_2 on the coal surface and has little effect on the adsorption of CH_4 , indicating that it was unfavorable for CO_2 to displace CH_4 at this time. From the fitted data, the variation law of saturation adsorption of both with moisture content is also basically consistent with the above analysis, so it can be inferred that the moisture content of 1 % or 5 % is unfavorable for CO_2 to displace CH_4 , and the

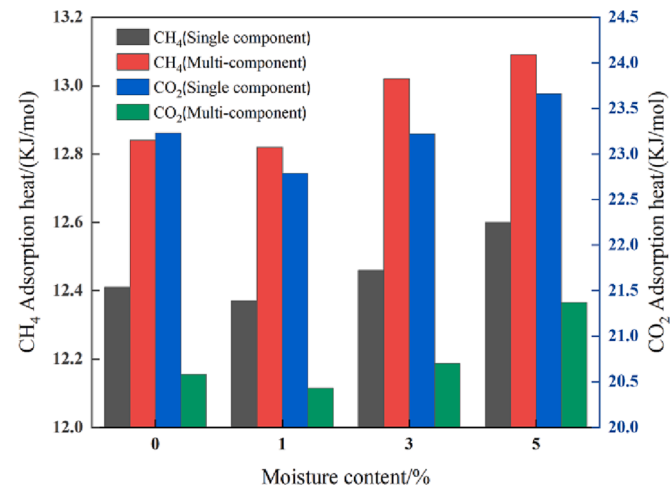


Fig. 8. Average isosteric adsorption heat of CH_4 and CO_2 at different moisture content.

moisture content of 3 % is favorable for CO_2 to displace CH_4 .

Fig. 8 shows the average equivalent heat of adsorption of CH_4 and CO_2 under different moisture content conditions. The average heat of adsorption of CH_4 and CO_2 slightly decreased from 0 % to 1 % moisture content, and the decrease of CO_2 was more obvious than that of CH_4 , which proved that the presence of H_2O at this time is unfavorable to the adsorption of CO_2 . The average heat of adsorption of CH_4 and CO_2 kept increasing from 1 % to 5 % moisture content. When there are fewer H_2O molecules, the high-energy adsorption sites are occupied by H_2O molecules preferentially due to the adsorption advantage of H_2O molecules

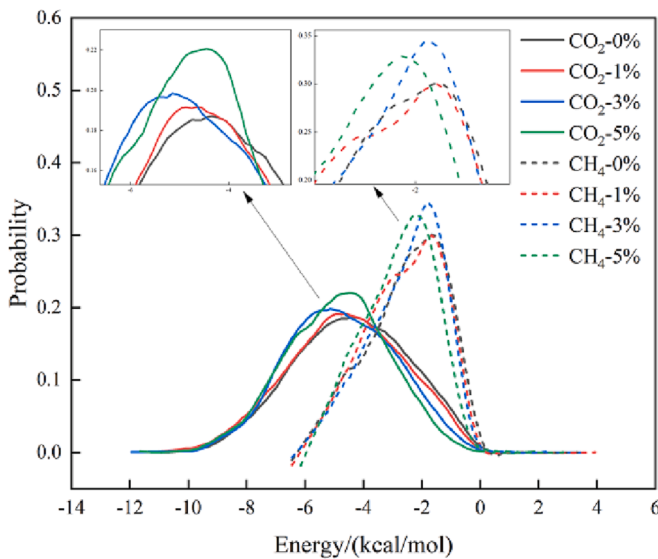


Fig. 9. Energy distribution with different moisture content.

in coal, and H₂O molecules compete with CH₄ and CO₂ for adsorption, and the heat of adsorption of both decreases. When there are more and more H₂O molecules, they will form different polyhedral clusters due to coalescence, and the formation of H₂O clusters will generate heat, and CH₄ molecules may generate hydrated molecules with H₂O molecules to release heat, and CO₂ molecules combine with H₂O molecules to form carbonic acid to generate heat [45], which makes the heat of adsorption of CH₄ and CO₂ increase.

4.2. Multi-component gas adsorption energy distribution

Fig. 9 shows the adsorption energy distribution of CH₄ and CO₂ at different moisture contents. Compared with CH₄, the adsorption energy curve of CO₂ has a wider distribution, which indicates that CO₂ has more adsorption sites on the coal surface and a larger adsorption range. The energy distribution of CO₂ shifted slightly to the left at the moisture content from 0 % to 1 %, which combined with the change of adsorption amount can indicate that when a small amount of H₂O molecules existed, the H₂O molecules occupied some of the high-energy adsorption sites, making the adsorption sites originally belonging to CO₂ less, but

the absolute value of the adsorption energy of the remaining CO₂ increased as a whole. The energy distribution of CH₄ remained basically unchanged at the highest peak, indicating that the presence of small amounts of H₂O molecules did not affect the adsorption of most CH₄. From the energy of CO₂ and CH₄ molecules becomes higher, it can be found that H₂O molecules have some binding ability to CO₂ or CH₄ molecules. When the moisture content is from 1 % to 3 %, the energy distribution of CO₂ is obviously shifted to the left, the adsorption is more stable, and the adsorption amount is also rising. At this time, a certain number of H₂O clusters are formed, and in addition to the adsorption of CO₂ molecules on the coal surface, the high potential of H₂O clusters also attracts CO₂ molecules. At this time, the overall energy distribution of CH₄ becomes narrower and more concentrated, indicating that the adsorption sites of CH₄ become less at this time, and the high potential of H₂O clusters tends to attract CO₂ molecules with higher electrostatic potential rather than CH₄. When the moisture content reaches 5 %, a large number of H₂O molecules form a H₂O molecule layer, which hinders the adsorption and diffusion of CO₂ and CH₄, but the H₂O molecules can still interact with CO₂ molecules. The energy of these CO₂ molecules is slightly lower than that of 3 % moisture content, but higher than that of 0 % and 1 % moisture content. At the same time, the presence of H₂O molecular layer also makes the H₂O molecules interact with CH₄ molecules, making the energy distribution shift to the left.

4.3. Entropy properties of gas adsorption

Entropy measures the degree of disorder in a system, and the adsorption entropy ΔS can be calculated through the Gibb-Helmholtz equation [51].

$$\Delta S = (\Delta H - \Delta G)/T \quad (3)$$

where the loss of ΔG (Gibbs free energy) can in turn be defined as the adsorption potential energy.

$$\varepsilon = -\Delta G \quad (4)$$

POLANYI [52] proposed the theory of adsorption potential energy and established the relationship between adsorption potential energy and pressure.

$$\varepsilon = RT\ln(p_s/p) \quad (5)$$

where, ε is the adsorption potential energy, J/(mol·K); T is the temperature, K; p_s is the gas saturation vapor pressure corresponding to the

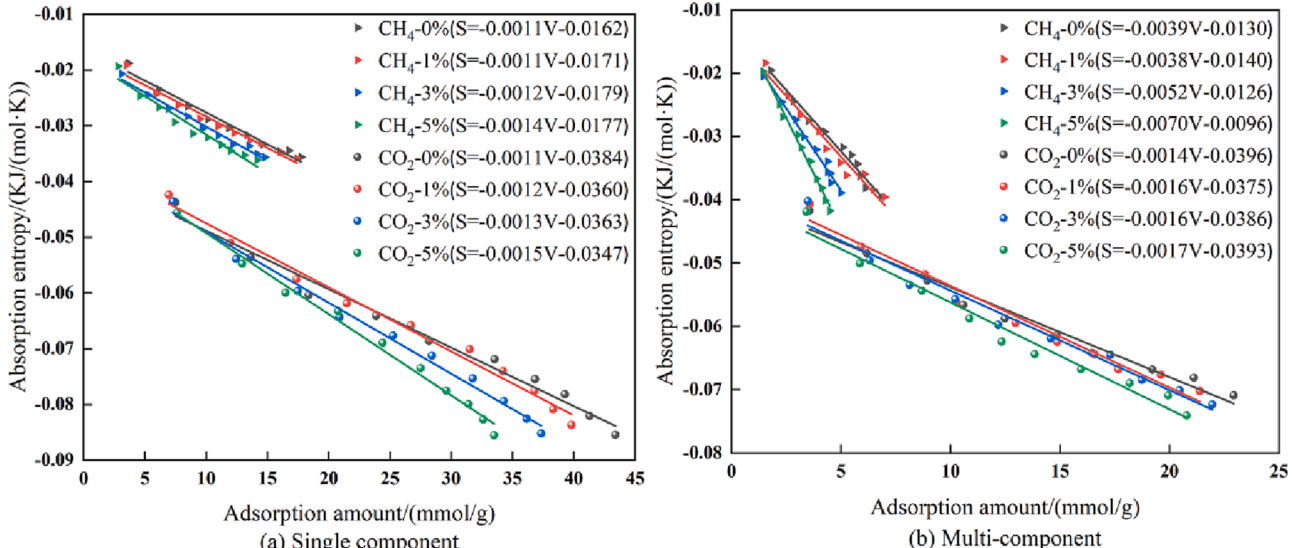


Fig. 10. The relationship between adsorption capacity and adsorption entropy at different moisture content.

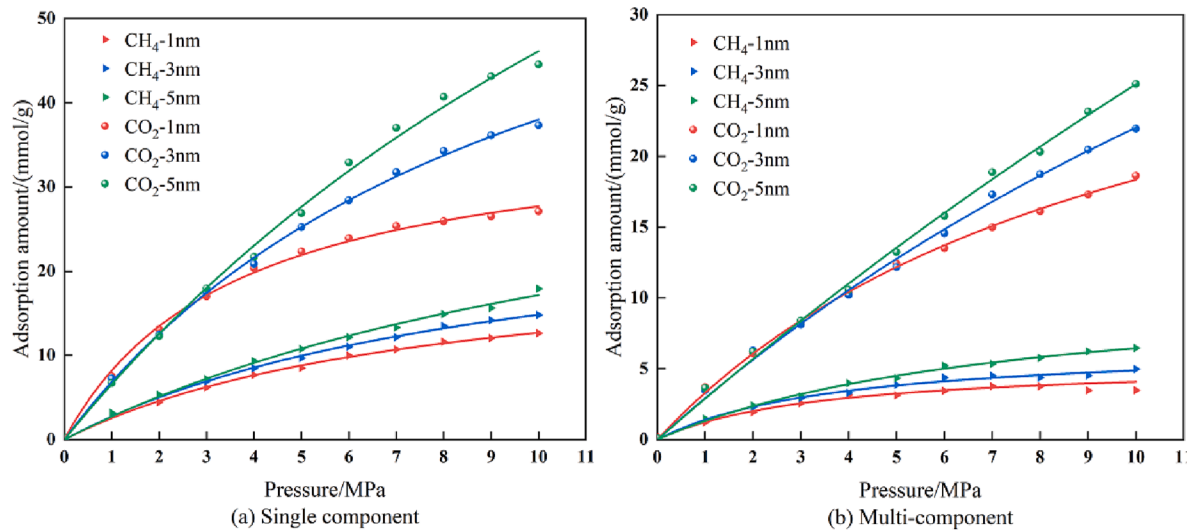


Fig. 11. Isothermal adsorption curves of CH₄/CO₂ with different pore sizes.

temperature T , MPa; R is the ideal gas constant, taken as 8.314 J/(mol·K).

DUBININ [53] established by statistical analysis of a large number of adsorption test data the formula for p_s .

$$p_s = p_c(T/T_c)^2 \quad (6)$$

where, p_c is the critical pressure, MPa; T_c is the critical temperature, K; CH₄ critical pressure is taken as 4.60 MPa, and the critical temperature is taken as 190.38 K; CO₂ critical pressure is taken as 7.38 MPa, and the critical temperature is taken as 303.98 K.

The calculated ΔH (enthalpy of adsorption) and ΔG (Gibbs free energy) can be substituted into equation (3) to obtain the adsorption entropy corresponding to different water contents, and a linear fit of the relationship curve between the adsorption amount and the adsorption entropy is shown in Fig. 10.

From Fig. 10, it can be seen that the adsorption entropy of CH₄ and CO₂ decreases with the increase of moisture content. The slope of the fitted curve of CH₄ is becoming smaller when two-component injection is made, and the change from 1 % moisture content to 3 % moisture content is more obvious, implying that the CH₄ molecules in the middle of the pore space are decreasing, while the slope of the fitted curve of CO₂ does not change much from 1 % moisture content to 3 % moisture content, indicating that the CO₂ molecules in the middle of the pore are not decreasing. The slope of the fitted curve of adsorption entropy represents how quickly the system reaches stability and how fast it reaches adsorption equilibrium. An important factor affecting the adsorption equilibrium is the number of gas molecules in the middle of

the pore space. If the absolute value of the slope of the curve is larger, it means that the equilibrium speed is faster and the number of gas molecules in the middle of the pore size is smaller. Combined with the above adsorption amounts, the adsorption of CH₄ decreases from 1 % moisture content to 3 % moisture content, and CO₂ increases, adding that the CO₂ at this time mainly displaces the CH₄ molecules in the middle of the pore space.

5. Effect of pore size on the thermodynamic properties of CH₄ and CO₂ adsorption

5.1. Gas adsorption capacity and thermal properties of adsorption

Fig. 11 shows the variation curves of CH₄ and CO₂ adsorption with injection pressure for different pore sizes, which are fitted using the Langmuir equation. Meanwhile, the density distribution of two-component adsorption of CH₄ and CO₂ at different pore sizes can be obtained by simulation as shown in Fig. 13.

From Fig. 11, it can be seen that as the pore size increases, more gas molecules can be accommodated between coal molecules, which makes the adsorption of CH₄ increase. And the adsorption of CO₂ is more at 1 nm than 3 nm and 5 nm when the pressure is less than 3 MPa, and after that it is positively correlated with the pore size. Since there are two states of existence of gas molecules in the slit model, one is adsorbed on the coal surface and the other is adsorbed in the middle of the pores. When the pressure is small, gas molecules are preferentially adsorbed on the high-energy adsorption sites on the coal surface, and as the pressure

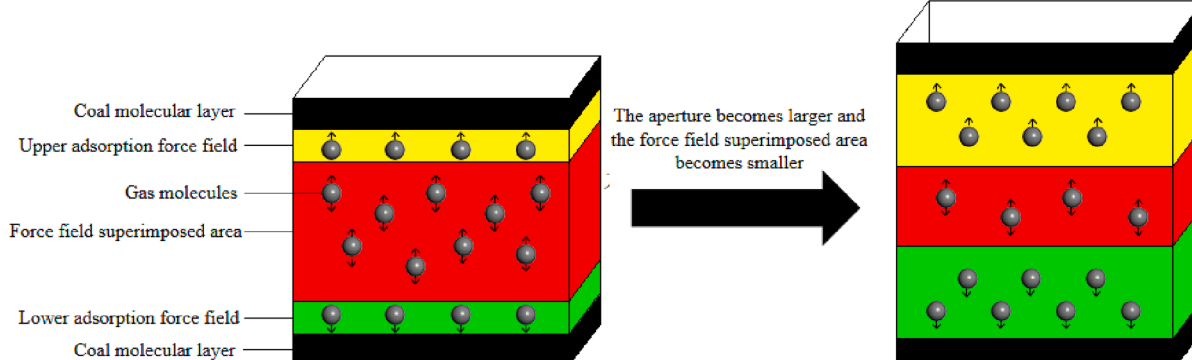


Fig. 12. Diagram of wall superimposed effect.

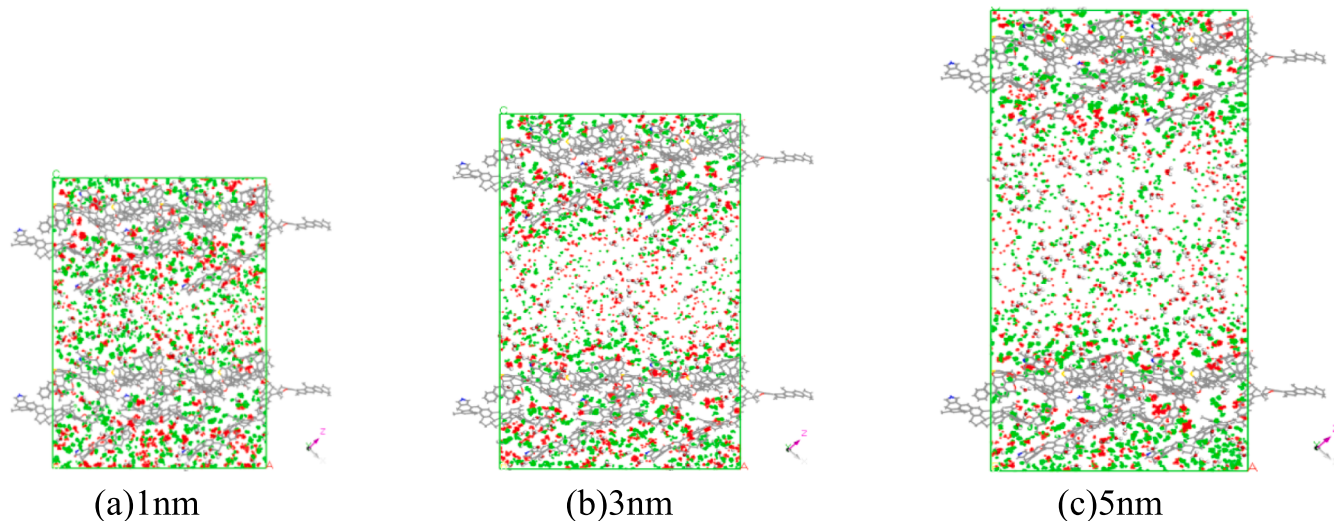


Fig. 13. Density distribution of CH₄ and CO₂ adsorbed by two components with different pore sizes (red represents CH₄, green represents CO₂). (For interpretation of the references to colour in this figure legend, the reader is referred to the web version of this article.)

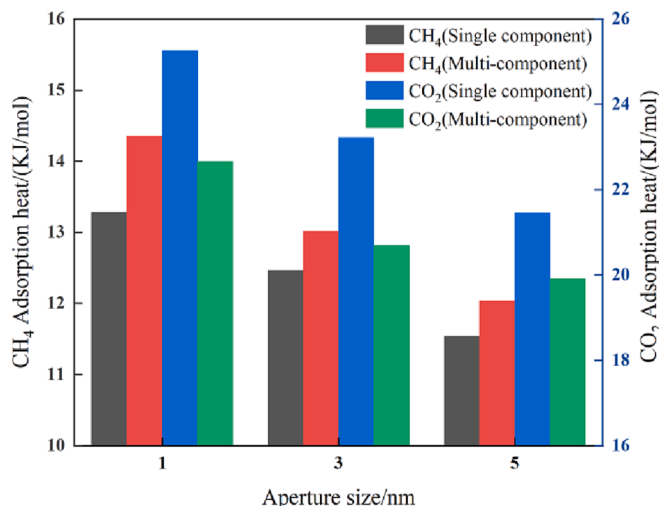


Fig. 14. Average equivalent heat of adsorption of CH₄/CO₂ with different pore sizes.

increases, more gas molecules are confined in the middle of the pores and cannot escape. The theory of adsorption potential by Polonyi [54–56] states that the adsorption process is the coalescence of adsorbent molecules under the action of force fields on the adsorbent surface. In microporous structures, due to the small spacing of the pore walls, the residual force field on their surfaces produces a superposition effect, which forms a superposition force field region within the microporous pore, causing the adsorbent molecules to coalesce uniformly inside the pore diameter, not just covering the inner wall surface, and this effect can also be called the wall superimposed effect (as shown in Fig. 12). When the pore size is small, the gas molecules are uniformly distributed throughout the pore space because of the wall superimposed effect, and as the pore size increases, the wall effect weakens and the gas molecules in the free space become sparse (as shown in Fig. 13). The wall superimposed effect is stronger for the 1 nm pore size, which makes the CO₂ gas molecules rapidly fill up the entire pore space. In contrast, the wall superimposed effect of 3 nm and 5 nm is weaker, but the free space is larger, so at less than 3 MPa, the CO₂ adsorption of 1 nm pore size is temporarily higher than that of 3 nm and 5 nm. In two-component adsorption, the increase of CH₄ adsorption from 3 nm to 5 nm is larger than that from 1 nm to 3 nm, while the increase of CO₂ is the

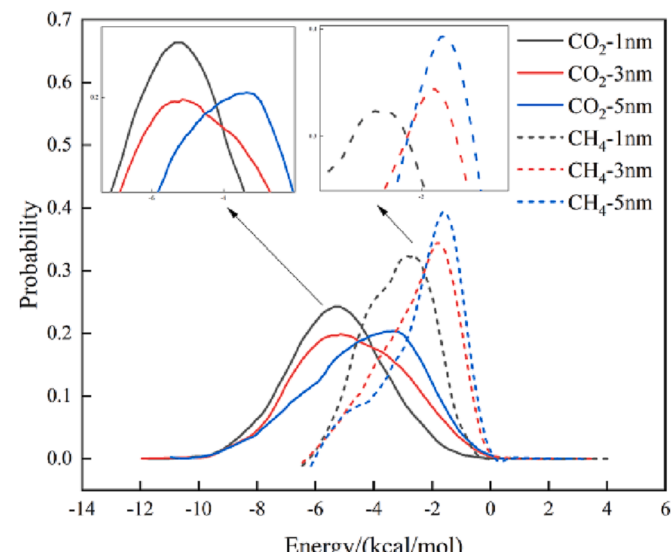


Fig. 15. Adsorption energy distribution with different pore sizes.

opposite, indicating that with the increase of pore size, the CO₂ in the competitive adsorption selectivity is decreasing.

Fig. 14 shows the average equivalent heats of adsorption of CH₄ and CO₂ for different pore sizes. It can be seen that the average heat of adsorption of both CH₄ and CO₂ decreases with increasing pore size, although the amount of adsorption of CH₄ and CO₂ is increasing at this time, but their magnitudes are different. The pore size is increasing exponentially while the adsorption volume is only slightly increasing, so the increase in free space is more significant compared to the increase in adsorption volume, which makes the intermolecular interactions weaker and the heat of adsorption decreases.

5.2. Multi-component gas adsorption energy distribution

Fig. 15 shows the adsorption energy distribution of CH₄ and CO₂ injected simultaneously at different pore sizes. Among them, the energy distribution of CO₂ has the highest absolute value of overall energy at 1 nm. In the 1 nm pore size, the force field superposition makes the adsorption of CO₂ molecules more stable and the absolute value of adsorption energy is larger, and similarly, the adsorption energy of CH₄

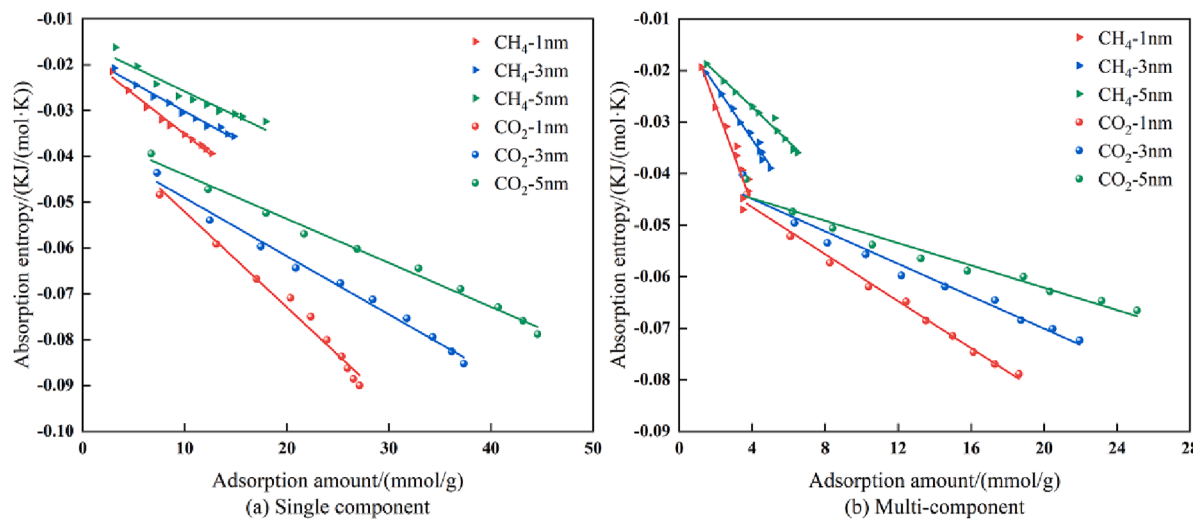


Fig. 16. Adsorption capacity versus entropy with different pore sizes.

molecules is also the highest at 1 nm. When the pore size is 3 nm, the wall superimposed effect becomes weaker, the activity space of molecules becomes larger, and the absolute value of adsorption energy of CH_4 and CO_2 becomes smaller. It is known from the adsorption amount that the adsorption selectivity of CO_2 decreases with the increase of pore size, and the diffusion ability of CO_2 is stronger than that of CH_4 , so the CO_2 molecules are more widely distributed and the energy is more dispersed in the pore size. When the pore size is 5 nm, the absolute values of adsorption energy of CO_2 and CH_4 continue to become smaller, but the change of CO_2 is greater.

5.3. Entropy properties of gas adsorption

Fig. 16 shows the variation curves of the entropy of CH_4 and CO_2 adsorption with the adsorption amount for different pore sizes.

As shown in Fig. 16, the entropy of adsorption of both CH_4 and CO_2 increases with the increase of pore size. As mentioned above, although the adsorption amount is increased, there is still a difference compared to the exponential increase of pore size, and the increased adsorption amount is also basically adsorbed in the free space, which is in the free state. The spatial extent of molecular activity becomes larger, and the disorder of the whole system increases, thus showing an increase in adsorption entropy.

6. Conclusion

- (1) The adsorption of CH_4 and CO_2 is negatively correlated with the moisture content, and positively correlated with the pore size. When two-component injection, with the increase of water content, the effect of CO_2 displacement CH_4 is also changing. 1 % or 5 % of water content is unfavorable to CO_2 displacement CH_4 , and 3 % of water content is favorable to CO_2 displacement CH_4 . With the increase of pore size, the selectivity of CO_2 in competitive adsorption is decreasing, and the effect of CO_2 displacement CH_4 is getting worse.
- (2) The average heat of adsorption of CH_4 and CO_2 was negatively correlated with the pore size and firstly decreased and then increased with the moisture content. The comparative analysis of the average heat of adsorption of CH_4 and CO_2 with different moisture contents shows that the effect of H_2O on CO_2 is stronger than that of CH_4 .
- (3) The adsorption energy distribution of CH_4 and CO_2 shows a wider distribution of CO_2 , indicating that CO_2 has more adsorption sites on the coal surface. With the increase of moisture content, the

absolute value of adsorption energy increases overall, and the high potential of H_2O clusters tends to attract CO_2 molecules more. With the increase of pore size, the wall superimposed effect is weakened, which makes the overall absolute value of adsorption energy smaller.

- (4) The adsorption entropy of CH_4 and CO_2 was negatively correlated with the moisture content and positively correlated with the pore size. The comparison of the slope of the fitted curves of the adsorption entropy at different moisture contents added that CO_2 mainly displaced the CH_4 molecules in the middle of the pore at 3 % moisture content.

CRediT authorship contribution statement

Ziwen Li: Methodology, Supervision, Funding acquisition. Yansong Bai: Formal analysis, Data curation, Writing – original draft. Hongjin Yu: Visualization, Investigation. Hongqing Hu: Writing – review & editing. Yinji Wang: Validation.

Declaration of Competing Interest

The authors declare that they have no known competing financial interests or personal relationships that could have appeared to influence the work reported in this paper.

Data availability

The authors do not have permission to share data.

Acknowledgements

The authors gratefully acknowledge the financial supports of the National Natural Science Foundation of China (52004176), the Research Project Supported by Shanxi Scholarship Council of China (2022-053), the Supported by Scientific and Technological Innovation Programs of Higher Education Institutions in Shanxi (2019L0246), the Supported by Fundamental Research Program of Shanxi Province (202203021211160) and the Supported by Postgraduate Teaching Reform Project of Shanxi Province (2022YJJG039).

References:

- [1] Chen L, Huang DB, Wang SY, Nie YN, He YL, Tao WQ. A study on dynamic desorption process of methane in slits. Energy 2019;175:1174–80. <https://doi.org/10.1016/j.energy.2019.03.148>.

- [2] Qin L, Wang P, Li S, Lin H, Wang R, Wang P, et al. Gas adsorption capacity changes in coals of different ranks after liquid nitrogen freezing. *Fuel* 2021;292:120404. <https://doi.org/10.1016/j.fuel.2021.120404>.
- [3] Qin L, Ma C, Li S, Lin H, Wang P, Long H, et al. Mechanical damage mechanism of frozen coal subjected to liquid nitrogen freezing. *Fuel* 2022;309:122124. <https://doi.org/10.1016/j.fuel.2021.122124>.
- [4] International Energy Agency (IEA), 2019. <https://www.iea.org/geco/data/>.
- [5] Li S, Ni G, Baisheng N, Shouqing Lu, Li X, Gang W. Microstructure characteristics of lignite under the synergistic effect of oxidizing acid and ionic liquid [Bmim][Cl]. *Fuel* 2021;289:119940. <https://doi.org/10.1016/j.fuel.2021.119940>.
- [6] Jia L, Li K, Shi X, Zhao L, Linghu J. Application of gas wettability alteration to improve methane drainage performance: A case study. *Int J Min Sci Technol* 2021;31(4):621–9. <https://doi.org/10.1016/j.ijmst.2021.04.000>.
- [7] Ni G, Hui W, Baisheng N, Yan W, Haoran D, Shouqing Lu, et al. Research of wetting selectivity and wetting effect of imidazole ionic liquids on coal. *Fuel* 2021;286:119331. <https://doi.org/10.1016/j.fuel.2020.119331>.
- [8] Guo X, Deng C, Fan Y, Fan N, Mu Y. Experimental study on leaf vein bionic gas drainage of multi-branch horizontal wells in coal seams. *Chin J Rock Mech Eng* 2019;38(12):2418–27.
- [9] Rodrigues de Brito MA, Baidya B, Ghoreishi-Madiseh SA. Techno-economic feasibility assessment of a diesel exhaust heat recovery system to preheat mine intake air in remote cold climate regions. *Int J Min Sci Technol* 2020;30(4):517–23.
- [10] Wang G, Qin X, Han D, Liu Z. Study on seepage and deformation characteristics of coal microstructure by 3D reconstruction of CT images at high temperatures. *Int J Min Sci Technol* 2021;31(2):175–85.
- [11] Mu Y, Fan Y, Wang J, Fan N. Numerical study on injection of flue gas as a heat carrier into coal reservoir to enhance CBM recovery. *J Nat Gas Sci Eng* 2019;72:103017. <https://doi.org/10.1016/j.jngse.2019.103017>.
- [12] Fan C, Elsworth D, Li S, Chen Z, Luo M, Song Yu, et al. Modelling and optimization of enhanced coalbed methane recovery using CO₂/N₂ mixtures. *Fuel* 2019;253:1114–29. <https://doi.org/10.1016/j.fuel.2019.04.158>.
- [13] Busch A, Gensterblum Y. CBM and CO₂-ECBM related sorption processes in coal: A review. *Int J Coal Geol* 2011;87(2):49–71.
- [14] van Bergen F, Tambach T, Pagnier H. The role of CO₂-enhanced coalbed methane production in the global CCS strategy. *Energy Proc* 2011;4(C):3112–6.
- [15] Pan Ye, Zhou T, Connell F. CO₂ storage in coal to enhance coalbed methane recovery: a review of field experiments in China. *Int Geol Rev* 2018;60(5–6):754–76.
- [16] Fujioka M, Yamaguchi S, Nakao M. CO₂-ECBM field tests in the Ishikari Coal Basin of Japan. *Int J Coal Geol* 2010;82(3–4):287–98.
- [17] Tarkowski R, Ułasz-Misiak B. Possibilities of CO₂ sequestration by storage in geological media of major deep aquifers in Poland. *Chem Eng Res Des* 2006;84(9):776–80.
- [18] van Wageningen WFC, Wentink HM, Otto C. Report and modeling of the MOVECBM field tests in Poland and Slovenia. *Energy Procedia* 2009;1(1):2071–8.
- [19] Wong S, Macdonald D, Andrei S, Gunter WD, Deng X, Law D, et al. Conceptual economics of full scale enhanced coalbed methane production and CO₂ storage in anthracitic coals at South Qinshui basin, Shanxi, China. *Int J Coal Geol* 2010;82(3–4):280–6.
- [20] Bachu S, Bonijoly D, Bradshaw J, Burruiss R, Holloway S, Christensen NP, et al. CO₂ storage capacity estimation: Methodology and gaps. *Int J Greenhouse Gas Control* 2007;430–43.
- [21] Clarkson CR, Bustin RM. The effect of pore structure and gas pressure upon the transport properties of coal: a laboratory and modeling study. 1. Isotherms and pore volume distributions. *Fuel* 1999;78(10):1333–44.
- [22] Fulton PF, Parente CA, Rogers BA, Shah N, Reznik AA. A laboratory investigation of enhanced recovery of methane from coal by carbon dioxide injection. Symposium on Unconventional Gas Recovery held in Pittsburgh, SPE 8930. 1981.
- [23] Reznik AA, Singh PK, Foley WL. An Analysis of the Effect of CO₂ Injection on the Recovery of In-Situ Methane From Bituminous Coal. An Experimental Simulation SPE 10822. 1984.
- [24] Busch A, Gensterblum Y. CBM and CO₂-ECBM related sorption processes in coal: a review. *Int J Coal Geol* 2011;87:49–71.
- [25] Bustin RM, Clarkson CR. Geological controls on coalbed methane reservoir capacity and gas content. *Int J Coal Geol* 1998;38:3–26.
- [26] Faiz M, Saghaei A, Sherwood N, Wang I. The influence of petrological properties and burial history on coal seam methane reservoir characterisation, Sydney Basin, Australia. *Int J Coal Geol* 2007;70:193–208.
- [27] Laxminarayana C, Crosdale PJ. Role of coal type and rank on methane sorption characteristics of Bowen Basin, Australia coals. *Int J Coal Geol* 1999;40:309–25.
- [28] Weniger P, Kalkreuth W, Busch A, Krooss BM. High-pressure methane and carbon dioxide sorption on coal and shale samples from the Parána Basin, Brazil. *Int J Coal Geol* 2010;84:190–205.
- [29] Zhang J, Clennell MB, Dewhurst DN, Liu K. Combined Monte Carlo and molecular dynamics simulation of methane adsorption on dry and moist coal. *Fuel* 2014;122:186–97.
- [30] Dang Y, Zhao L, Lu X, Xu J, Sang P, Guo S, et al. Molecular simulation of CO₂/CH₄ adsorption in brown coal: effect of oxygen-, nitrogen-, and sulfur-containing functional groups. *Appl Surf Sci* 2017;423:33–42.
- [31] Li Y, Yang Z, Li X. Molecular simulation study on the effect of coal rank and moisture on CO₂/CH₄ competitive adsorption. *Energy Fuel* 2019;33:9087–98.
- [32] Liu XQ, He X, Qiu NX, Yang X, Tian ZY, Li MJ, et al. Molecular simulation of CH₄, CO₂, H₂O and N₂ molecules adsorption on heterogeneous surface models of coal. *Appl Surf Sci* 2016;389:894–905.
- [33] Long H, Lin H-F, Yan M, Bai Y, Tong X, Kong X-G, et al. Adsorption and diffusion characteristics of CH₄, CO₂, and N₂ in micropores and mesopores of bituminous coal: molecular dynamics. *Fuel* 2021;292:120268.
- [34] Zhang J, Liu K, Clennell MB, Dewhurst DN, Pervukhina M. Molecular simulation of CO₂-CH₄ competitive adsorption and induced coal swelling. *Fuel* 2015;160:309–17.
- [35] Cracknell RF, Nicholson D, Quirk N. A grand canonical Monte Carlo study of Lennard-Jones mixtures in slit shaped pores. *Mol Phys* 1993;80(4):885–97.
- [36] Cracknell RF, Nicholson D, Quirk N. A grand canonical Monte-Carlo study of Lennard-Jones mixtures in slit pores; 2: mixtures of two centre ethane with methane. *Mol Simul* 1994;13(3):161–75.
- [37] You J, Tian L, Zhang C, et al. Adsorption Behavior of Carbon Dioxide and Methane in Bituminous Coal: A Molecular Simulation Study. *Chin J Chem Eng* 2016;24:1275–82.
- [38] Xiang JH, Zeng FG, Liang HZ, et al. Molecular simulation of the CH₄/CO₂/H₂O adsorption onto the molecular structure of coal. *Sci China: Earth Sci* 2014;44(07):1418–28. <https://doi.org/10.1007/s11430-014-4849-9>.
- [39] Shugang LI, Yang BAI, Haifei LIN, et al. Molecular simulation of adsorption thermodynamics of multicomponent gas in coal. *J China Coal Soc* 2018;43(9):2476–83. <https://doi.org/10.13225/j.cnki.Jccs.2017.1851>.
- [40] Zhao J, Deng S, Zhao Li, Zhao R. CO₂ Adsorption Capture in Wet Gas Source: CO₂/H₂O Co-Adsorption Mechanism and Application. *Prog Chem* 2022;34(03):643–64.
- [41] Jiakang SI. Macromolecular structure model construction and molecular simulation of Malan8 coal. Taiyuan University of Technology; 2014.
- [42] Kruse H, Grimmelmeier S. A geometrical correction for the inter- and intra-molecular basis set superposition error in Hartree-Fock and density functional theory calculations for large systems. *J Chem Phys* 2012;136(15):154101.
- [43] Murray JS, Politzer P. The electrostatic potential: an overview. *Wiley Interdiscip Rev Comput Mol Sci* 2011;1(2):153–63.
- [44] Li Z, Ni G, Wen Y, Jiang H, Zhang X, Wang G, et al. Coal-CH₄/CO₂ high-low orbit adsorption characteristics based on molecular simulation. *Fuel* 2022;315.
- [45] Jinxiun HAN. Molecular simulation of gas adsorption and desorption-diffusion in the aqueous coal. Southwest Petroleum University; 2015.
- [46] Zhang JF, Clennell MB, Dewhurst DN, et al. Combined Monte Carlo and molecular dynamics simulation of methane adsorption on dry and moist coal. *Fuel* 2014;122:186–97.
- [47] Billemont P, Coasne B, De Weireld G. An experimental and molecular simulation study of the adsorption of carbon dioxide and methane in nanoporous carbons in the presence of water. *Langmuir* 2011;27(3):1015–24.
- [48] Purdie MJ, Qiao Z. Molecular simulation study of wet flue gas adsorption on zeolite 13X. *Microporous Mesoporous Mater* 2018;261:181–97.
- [49] Gang Li, Penny Xiao, Paul Webley. Binary adsorption equilibrium of carbon dioxide and water vapor on activated alumina. *Langmuir* 2009;25(18):10666–75.
- [50] Hongqing Zhu, Zhang Yilong Hu, Lintao Liao Qi, Shuhao Fang, Rongxiang Gao. Dynamic Simulation Based on a Simplified Model of 1/3 Coking Coal Molecule and Its Formation Characteristics of Hydration Films. *ACS Omega* 2021;6(49):33339–53.
- [51] Matthias PM, O'Connell JP. The Gibbs-Helmholtz Equation and the Thermodynamic Consistency of Chemical Absorption Data. *Ind Eng Chem Res* 2012;51(13):5090–7.
- [52] Polanyi M. The Potential Theory of Adsorption. *Science* 1963;141(3585):1010–3.
- [53] Dubinin MM. The Potential Theory of Adsorption of Gases and Vapors for Adsorbents with Energetically Nonuniform Surfaces. *Chem Rev* 1960;60(2):235–41.
- [54] Polanyi M. Theories of the Adsorption of Gases: A General Survey and Some Additional Remarks. *Trans Faraday Soc* 1932;28:316.
- [55] Do DD, Do HD. Adsorption of Supercritical Fluids in Non-porous and Porous Carbons: Analysis of Adsorbed Phase Volume and Density. *Carbon* 2003;41(9):1777–91.
- [56] Elliott JR, Suresh SJ, Donohue MD. A Simple Equation of State for Nonspherical and Associating Molecules. *Ind Eng Chem Res* 1990;29(7):1476–85.